Bull. Mater. Sci., Vol. 33, No. 6, December 2010, pp. 713–717. © Indian Academy of Sciences.

Synthesis and properties of dental zirconia–leucite composites

MING KANG[1,2], XIAOMING LIAO[1], GUANGFU YIN[1*], XUN SUN[3], XING YIN[4], LU XIE[4] and JUN LIU[2]

[1]College of Materials Science and Engineering, Sichuan University, Chengdu 610064, China

[2]College of Material Science and Engineering, Southwest University of Science and Technology, Mianyang 621010, China

[3]Department of Urology, People's Hospital of Jinghong, Jinghong 666100, China

[4]West China College of Stomatology, Sichuan University, Chengdu 610041, China

MS received 11 May 2009; revised 11 July 2009

Abstract. **The dental zirconia–leucite composites were synthesized by high temperature solid-state method using potash feldspar, potassium carbonate and zirconia as raw materials. The mechanical properties and the coefficient of thermal expansion (CTE) of the prepared zirconia–leucite composites were tested. The results show that the bending strength, the fracture toughness and the metal–ceramic bonding strength of the prepared samples are about 110 MPa, 3·5 MPa/m$^{1/2}$ and 45 MPa, respectively. The CTE was about 13·73×10^{-6} °C^{-1} and close to that of Ni–Cr dental alloy (14·0×10^{-6} °C^{-1}). The results indicate that the introduction of zirconia is beneficial to the improvement in the mechanical properties and CTE adjustment of porcelain material. The clinical application of the zirconia–leucite composites with good metal–ceramic bonding strength in the dental restoration could be envisioned.**

Keywords. **Zirconia; leucite; metal–ceramic bond; mechanical properties.**

1. Introduction

Dental defect is a common trauma of the oral cavity, which not only impairs people's health but also does harm to people's appearance. Porcelain-fused to metal (PFM) teeth has been widely used in clinical restoration due to their characteristics such as natural beauty, obdurability, wear resistance and corrosion resistance (Dent *et al* 1982; Hacher *et al* 1996; Kelly *et al* 1996; Könönen and Kivilahti 2001; Almilhatti *et al* 2003). Published results show that about half of PFM teeth crack or collapse in the clinical application, largely as a result of the poor performance of the porcelain powder (Liu *et al* 2008). For example, metal substrate and ceramic powders cannot match very well with each other in the linear coefficient of thermal expansion (CTE). In addition to that, the corresponding adhesive capability, bending strength and fracture toughness cannot meet the actual requirements. Generally, the chemical or mineral raw materials are usually selected to prepare the porcelain powders. Firstly the raw materials are mixed with the appropriate nucleating agent. Then leucite, which is widely adopted as the reinforcing material of dental ceramics in the clinical use (Mackert *et al* 1996; Yin *et al* 2003; Cesar *et al* 2005), is synthesized after three-step thermal processing of melting, nucleation and crystallization (Mackert *et al* 2001). Leucite is usually added into the dental porcelain by the incongruent melting of potash feldspar or as a synthetic powder. The bulk of the porcelain is a glass matrix with a relatively small percentage of leucite crystal dispersed within it (Lee *et al* 2004). However, the preparation process is complicated and the synthetic conditions are difficult to control, which is unfavourable for this method. Research shows that many feldspar mineral materials such as feldspar, kaolinite, nepheline, zeolite and so on, which are similar to leucite in the component, can be transformed into leucite under high temperature (Hashimoto *et al* 2005). As is known, zirconia not only has superior mechanical properties and comparatively low CTE (about 9·0×10^{-6} °C^{-1}) in comparison with that of leucite (about 30×10^{-6} °C^{-1}), but also has good biocompatibility, chemical stability, non-sensitive, good aesthetics and so on. Except for that, it could go with gums and mucous membrane well to achieve the good effects (Brecker 1956; Weiscin and Weistein 1962; Sollazzo *et al* 2008). Hence, zirconia was introduced in the synthesis system to improve the mechanical properties and adjust CTE of the as-prepared ceramics to match the CTE of Ni–Cr alloy base (about 14·0×10^{-6} °C^{-1}). Ni–Cr alloys, which have still been widely used as the substrate for the restoration of teeth in some developing countries because of the economical and other reasons, were adopted in our study.

In this paper, zirconia–leucite composites were synthesized through high-temperature solid-state reaction using

*Author for correspondence (nic0700@scu.edu.cn)

potash feldspar, potassium carbonate and zirconia as raw materials. The mechanical properties of the obtained samples were examined on the electronic universal testing machine. The morphology, phase constituents, components and CTE were also characterized by scanning electron microscopy (SEM), X-ray diffraction (XRD), Raman spectroscopy, energy dispersive X-ray spectrometer (EDX) and thermal expansion instrument, respectively. The zirconia–leucite composites with good metal–ceramic bonding strength will have great potential in the clinical application of the dental porcelain restoration.

2. Experimental

2.1 *Synthesis of zirconia–leucite composites*

Zirconia–leucite composites were prepared through high-temperature solid-state reaction using potash feldspar (Qingyuan, China), analytical reagent potassium carbonate (K_2CO_3) and Y_2O_3-stabilized zirconia (ZrO_2, Jiankun Chemical Co., China) as the main raw materials. The potash feldspar is mainly composed of 67·62% SiO_2, 18·29% Al_2O_3 and 9·72% K_2O (wt%). As is known, 23% K_2O in leucite is much higher than that in potash feldspar. Hence, in order to adjust the ratio of potassium oxide and high-temperature melting performance, potassium carbonate was introduced in our experiment. In this paper, 22·39% K_2O and 8% ZrO_2 was employed. Briefly, a certain amount of potash feldspar, potassium carbonate and zirconia were first placed in a nylon tank with 95 alumina CERAMIC BALLS as the milling media and ethanol as the solvent. Then the mixed materials were put into QM-1SP planetary-type ball mill to obtain uniform mixture. After drying, the mixture was then transferred into corundum crucible and sintered at 1200 °C for 1 h followed by natural cooling to room temperature. Finally, the sintered products were ground, milled and screened to obtain zirconia–leucite composite ceramic powders.

2.2 *Characterization of zirconia–leucite composites*

The bars with a dimension of 30×5×5 mm were prepared by uniaxial pressing of the zirconia–leucite composite ceramic powders at a pressure of 20 MPa for 2 min and the compacts were sintered at 950 °C for 0·5 h followed by slow furnace cooling. The phase constituents and morphology of the as-prepared samples were investigated by X-ray diffraction (XRD, D/max-III B-type, Japan) and Raman (Renishaw, InVia, England), scanning electron microscopy (SEM, Hitachi TM-1000, Japan), respectively. In order to reveal the microstructure of the materials, the sample for SEM characterization was etched with 5% HF solution for 1 min and then cleaned with ultrasonic cleaning system for 10 min and dried for 24 h at room temperature. The CTE was measured by a Dilatometer (DIL402PC, Netzsch, Germany). The bending strength, fracture toughness and metal–ceramic bonding strength for the investigated samples were measured by an electronic universal testing machine (AG-IC 20KN, Shimadzu, Japan). The elemental distribution of the metal–ceramic interface was analysed by the attached EDX of Hitachi-S4800 SEM. The bending strength, fracture toughness and metal–ceramic bonding strength were measured based on three-point bending test. But for the fracture toughness test, the method of single-edge notch beam (SENB) was adopted. The bars, which were prepared by uniaxial pressing of the prepared porcelain powders at a pressure of 20 MPa for 2 min, were first cut into a blade-thin slit with a size of 0·2×2 mm, and the compacts were sintered at 950 °C for 0·5 h followed by slow furnace cooling. Although the nominal dimension of the samples was 30×5×5 mm, there were small variations in the real dimensions. Hence, width b and thickness h were measured and the bending strength δ_b can be calculated using (1). Fracture toughness, K_{IC}, can be obtained according to (2) and (3)

$$\sigma_b = 3PL/\left(2bh^2\right), \tag{1}$$

$$K_{IC} = Y\left\{3PL/\left(2bw^2\right)\right\}a^{1/2}, \tag{2}$$

$$Y = 1{\cdot}93 - 3{\cdot}07(a/w) + 14{\cdot}53(a/w)^2 - 25{\cdot}07(a/w)^3 + 258{\cdot}0(a/w)^4, \tag{3}$$

where P is the load at the time of fracture; L, w and a are span, thickness and depth of the incision of the investigated sample, respectively.

Metal–ceramic bonding strength was determined by the method used in the international standard ISO9693:1999. The Ni–Cr alloy was supplied by Sichuan University, whose CTE was about $14{\cdot}0\times10^{-6}$ °C^{-1} and elastic modulus, 210 GPa. Briefly, Ni–Cr alloy was machined to a sheet with a size of 25×5×0·5 mm followed by grinding, polishing, sand blasting, removal of air and clearance treatment to remove surface contaminants. The size of the samples for bonding strength test was in accordance with the size prescribed in ISO9693:1999. In order to evaluate the bonding strength, a certain amount of regulators was mixed into the powders and then coated evenly on the Ni–Cr alloy substrates with a brush. After drying and sintering at 960 °C for 0·5 h, all the testing samples were well prepared. The samples were placed on two fulcrums with the ceramic side downward. The fracture force F was obtained by the measurement of vertical force exerted in the mid point of the sample when the ceramic layer just broke. The value of the coefficient k as a function of metal substrate thickness, d_M and metal elastic modulus, E_M, was determined according to the international standard ISO9693:1999. The bonding strength, τ_b, was calculated according to the formula $\tau_b = k\times F$. All the experiments were carried out in quintuplicate. The results were presented as mean ± standard

deviation. Significant differences were determined by *t*-test. $P < 0{\cdot}05$ was considered to be significant.

3. Results and discussion

3.1 *Mechanical properties*

The bending strength, fracture toughness and the metal–ceramic bonding strength of samples are 109·93±7·01 MPa, 3·47±0·32 MPa/$m^{1/2}$ and 45·09±0·11 MPa, respectively, significantly higher than the corresponding value of 50 MPa, 2·5 MPa/$m^{1/2}$ and 25 MPa prescribed in ISO9693:1999 ($p < 0{\cdot}05$). The results indicate that the zirconia–leucite composites exhibit good mechanical properties.

3.2 *SEM analysis*

Figure 1 is the SEM photograph of hydrofluoric acid etched zirconia–leucite composites. From figure 1, it can be seen that a large number of tetragonal phase leucite crystals exists. A small amount of zirconia crystal with a size of about 0·5–2 μm scattered between the leucite crystals can also be observed.

According to the theory of Griffith, micro-cracks, when leucite grains evenly distribute in the glass phase, there are a lot of small cracks and defects in ceramic materials. Under the external stress, cracks begin to expand across the grain boundary or along the direction paralleling to the grain boundary, thus there is a big increase in the number of crack expansion paths, also in the resistance to crack expansion and helpful to improve the mechanical strength of ceramic materials.

3.3 *XRD and Raman analysis*

The XRD pattern and Raman spectroscopy of the composite powders are shown in figures 2 and 3, respectively. From figure 2, it can be seen that only diffraction peaks of zirconia (No. 49-1672) and leucite (No. 38-1423) are detected, indicating that the main crystal phases of the sample are zirconia and leucite crystal.

From figure 3, the characteristic peak of leucite crystal at 499·56 cm^{-1} in terms of the literature through the standard card (Renishaw ro2-S/NH 14030) can be observed. In addition, the tetragonal zirconia characteristic absorption peaks around 253·18, 463·79 and 642 cm^{-1} are detected (Grover *et al* 2007). Hence, it could be safely concluded that there is zirconia in the samples and the crystalline phase remained unchangeable, which is in line with the XRD analysis. In short, during the preparation of ceramic powders, zirconia crystal phase does not make any transformation, which is helpful to the increase of the fracture toughness. The reason is that the formation of the solid solution between some oxides (such as CaO and Al_2O_3) in the raw materials and ZrO_2 leads to the change of the internal structure of the zirconia crystal, which results in the

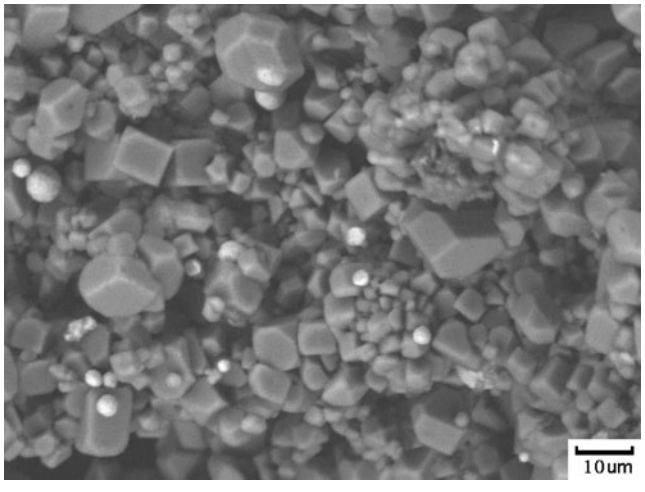

Figure 1. SEM photograph of hydrofluoric acid etched zirconia–leucite composites.

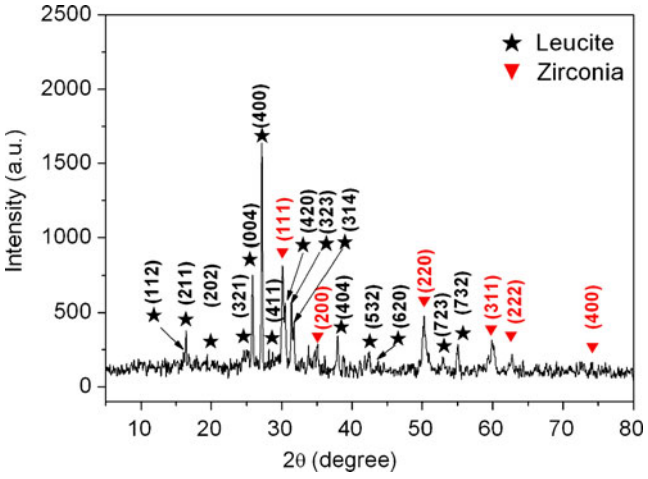

Figure 2. XRD pattern of zirconia–leucite composites.

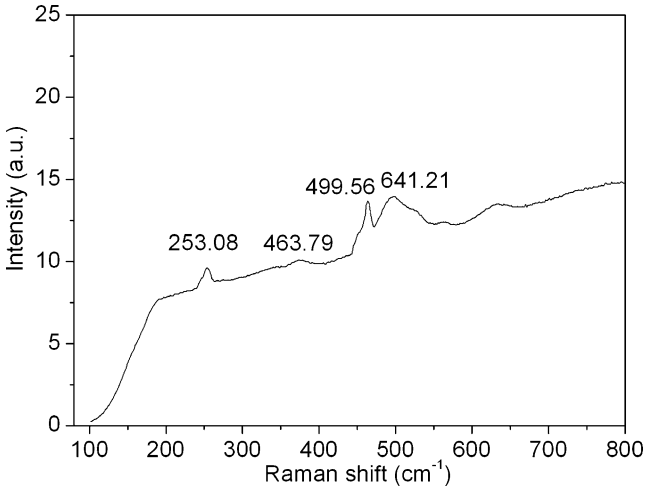

Figure 3. Raman spectra of zirconia–leucite composites.

increase of the chemical energy barrier of the transformation from tetragonal zirconia (*t*) to the monoclinic zirconia (*m*) and improves the stability of the *t*-phase, also subsequently decline the initial phase change temperature. Hence, metastable *t*-ZrO_2 can be retained at room temperature. When the external force is employed on the ceramic materials, martensitic phase transformation for metastable *t*-ZrO_2 will happen and consequently increase their toughness. As a result, the introduction of zirconia increased the fracture toughness to about 3·5 MPa/$m^{1/2}$, a 40% increase compared with the prescribed value (2·5 MPa/$m^{1/2}$) in ISO9693:1999.

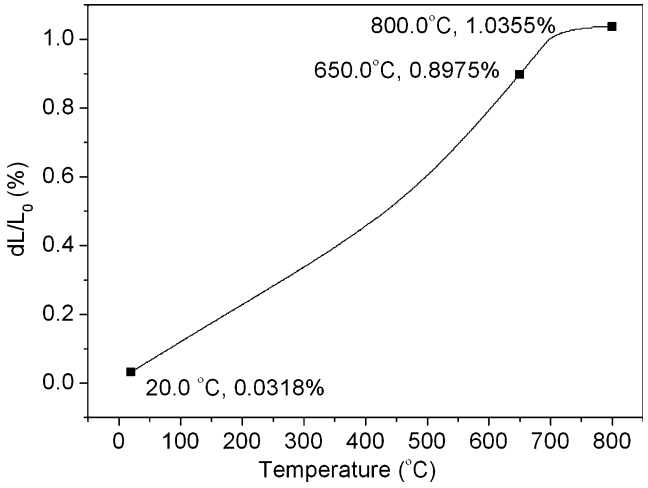

Figure 4. CTE curve of zirconia–leucite composites.

3.4 *CTE analysis*

CTE curve of the prepared zirconia–leucite composites is shown in figure 4. From figure 4, it can be seen that with the increasing temperature, the thermal expansion rate gradually increases and reaches to 0·031 %, 0·8975 % and 1·0355 % at 20 °C, 650 °C and 800 °C, respectively. There is linear expansion during the range of 20–650 °C. According to the formula, $\alpha = \Delta L/L_0 \times \Delta T \pm 5{\cdot}7 \times 10^{-7}$, the CTE of the samples is about $13{\cdot}75 \times 10^{-6}$ °C^{-1} and was close to that of the nickel–chromium alloy (about $14{\cdot}0 \times 10^{-6}$ °C^{-1}). This shows that the addition of zirconia is beneficial to the adjustment of CTE of ceramic materials and ensures the matching of the ceramic materials with nickel–chromium alloy substrate in the thermal expansion performance. From figure 4, it can also be observed that the CTE curve tends to be parallel above 800 °C, indicating that the CTE of ceramic materials remained unchangeable at higher temperature.

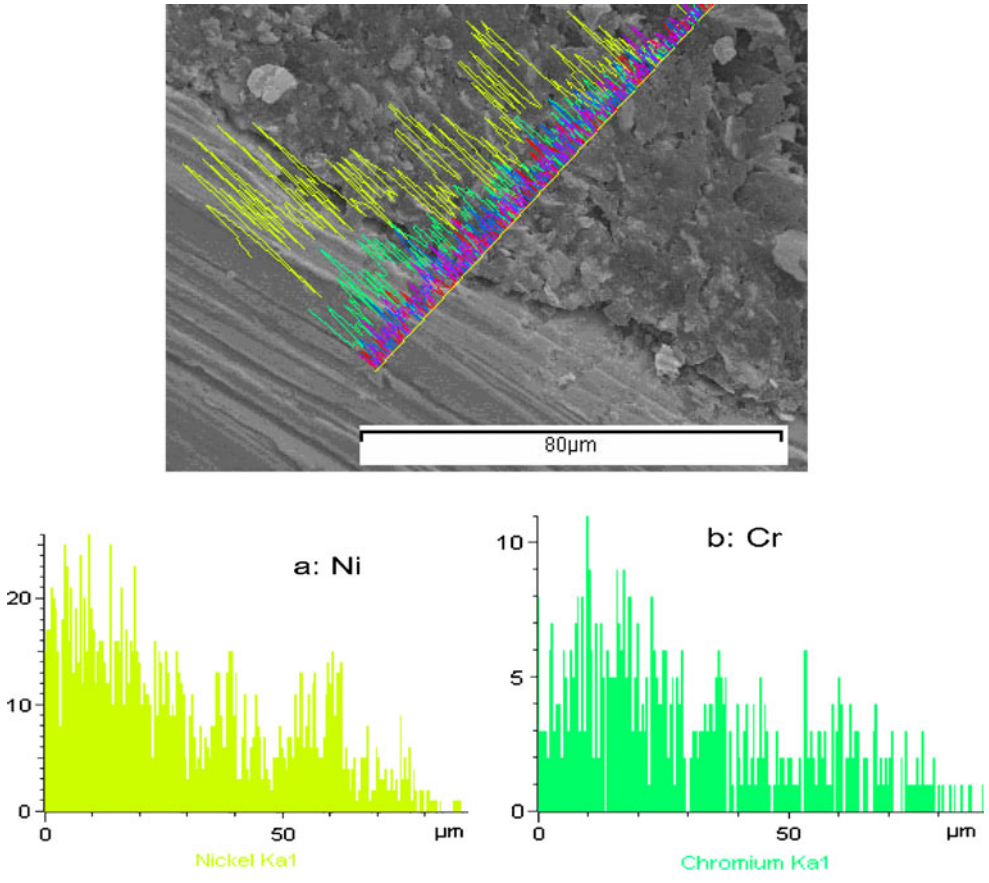

Figure 5. EDX spectra of the interface between Ni–Cr alloy and ceramic.

3.5 *Metal–ceramic interface analysis*

SEM was employed to examine the metal–ceramic interface and EDX test was used to investigate the elemental distribution along the direction from the metal layer to the ceramic layer (shown in figure 5). From figure 5, no obvious stratification between the metal and ceramic can be observed. In the EDX spectra, yellow, green, red, purple and blue curves were corresponding to content change of Ni, Cr, K, Si and Al elements, respectively, showing that the interdiffusion of atoms occurred during sintering. Among them, the distribution of the Ni and Cr elements was shown in figures 5a and b, respectively. It can be seen that the content of Ni and Cr elements decreases along the direction from the metal layer to the ceramic layer, indicating that Ni and Cr diffuse into the ceramic layer, especially the diffusion of element Ni is more remarkable. As is known to all, the reaction of metal–porcelain interfaces is complicated. In these complex systems, diffusion bond is established not only by mutual interdiffusion but also by simultaneous solid-state reactions (Hegedűs *et al* 2002; Liu *et al* 2008). The formation of compound interface, which mainly resulted from the dissolution and diffusion of the metal and ceramic powders with each other, is very favourable to the increase of metal–ceramic bonding strength. From the relationship between Gibbs free energy and temperature for the metal oxide (Steiner *et al* 1997), the Gibbs free energy of generating Cr_2O_3 is lower than that of Al_2O_3 at 1233·15 K (960 °C). That is to say, Cr has greater affinity with O than Al. Hence, Cr of Ni–Cr alloy can be dissolved and spread out to the porcelain interface when the ceramic powder was in a molten state. Meanwhile, it could substitute Al of Al_2O_3 in porcelain powder and consequently prompt the formation of Cr_2O_3. It has also been reported that a very thin Cr_2O_3 layer already exists on the surface of the Ni–Cr alloy at the start of the sintering process (Hegedűs *et al* 2002). On the other hand, the replaced Al and Ni may react and then $A1Ni_3$ is produced (Mackert *et al* 1996). These suggest that the interface is an integration of diffusion type and compound type, which acts as the transition layer between the Ni–Cr alloy layer and porcelain layer, thereby reducing interface defects and improving the adhesion strength of metal–ceramic interface. At the same time, the different layers of oxides also contribute to surface wetting effects of the molten porcelain on the surface of metal and consequently enhance the metal–ceramic bonding strength.

4. Conclusions

The dental zirconia–leucite composites were synthesized by high temperature solid-state method using potash feldspar, potassium carbonate and zirconium oxide as raw materials. The bending strength, the fracture toughness and the metal–ceramic bonding strength of the investigated sample are about 110 MPa, 3·5 $MPa/m^{1/2}$ and 45 MPa, respectively. The CTE was about $13{\cdot}73\times10^{-6}$ $°C^{-1}$ and close to that of Ni–Cr dental alloy ($14{\cdot}0\times10^{-6}$ $°C^{-1}$). The introduction of zirconia is beneficial to the improvement in the mechanical properties of the porcelain materials, and the matching of the CTE between the metal substrates and porcelain powders. The zirconia–leucite composites with good metal–ceramic bonding strength will have great potential in the clinical application of dental restoration.

Acknowledgements

This work was financially supported by the National Natural Science Foundation of China (10476024) and Science and Technology Bureau of Sichuan province (2006 J13-059). The support of the restoration centre for dental prosthetics, West China College of Stomatology of Sichuan University is also gratefully acknowledged.

References

Almilhatti H J, Giampaolo E T, Vergani C E, Machado A L and Pavarina A C 2003 *J. Dent.* **31** 205
Brecker C S 1956 *J. Prosthet. Dent.* **6** 801
Cesar P F, Yoshimura H N, Junior W G M and Okada C Y 2005 *J. Dent.* **33** 721
Dent R J, Preston J D, Moffa J P and Caputo A 1982 *J. Prosthet. Dent.* **47** 59
Grover V, Shukla R and Tyagi A K 2007 *Scr. Mater.* **57** 699
Hacher C H, Wagner W C and Razoog M E 1996 *J. Prosthet. Dent.* **75** 14
Hashimoto S, Sato F, Honda S, Hideo A and Fukuda K 2005 *J. Ceram. Soc. Jpn* **113** 488
Hegedűs C, Daróczi L, Kökényesi V and Beke D L 2002 *J. Dent. Res.* **81** 334
Kelly J R, Nishimura I and Campbell S D 1996 *J. Prosthet. Dent.* **75** 18
Könönen M and Kivilahti J 2001 *J. Dent. Res.* **80** 848
Lee Y K, Park H Y, Shim J E, Kim K N and Lee K W 2004 *J. Non-cryst. Solids* **349** 200
Liu J, Qiu X M, Zhu S and Sun D Q 2008 *Mater. Sci. Eng.* **A497** 421
Mackert J R, Khajotia S S, Russell C M and Williams A L 1996 *Dent. Mater.* **12** 8
Mackert J R, Twiggs S W, Russell C M and Williams A L 2001 *J. Dent. Res.* **80** 1574
Sollazzo V, Pezzetti F, Scarano A, Piattelli A, Bignozzi C A, Massari L, Brunelli G and Carinci F 2008 *Dent. Mater.* **24** 357
Steiner P J, Kelly R J and Giuseppetti A A 1997 *Int. J. Prosthodont.* **10** 375
Weiscin M and Weistein A B 1962 *US Patent* 3052983
Yin L, Jahanmir S and Ives L K 2003 *Wear* **255** 975